

DNA Synthesis Past a 5-MethylC-Containing *cis-syn*-Cyclobutane Pyrimidine Dimer by Yeast Pol η Is Highly Nonmutagenic[†]

Bich Vu, Vincent J. Cannistraro, Liping Sun, and John Stephen Taylor*

Department of Chemistry, Washington University, St. Louis, Missouri 63130

Received January 31, 2006; Revised Manuscript Received May 1, 2006

ABSTRACT: Cyclobutane pyrimidine dimers (CPDs) are responsible for a considerable fraction of sunlight-induced C to T and 5-methylcytosine (^mC) to T mutations in mammalian cells, though the precise mechanism is unknown. One possibility is that the C or ^mC of a CPD is not mutagenic and must first deaminate to U or T, respectively, for A to be inserted by a DNA polymerase. Alternatively, A might be directly inserted opposite the C or ^mC prior to deamination via an *E*-imino tautomer of the C or ^mC or by a nontemplated mechanism in which the photoproduct is sterically excluded from the active site. We have taken advantage of the retarding effect of C5 methylation on the deamination rate of *cis-syn*-cyclobutane dimers to prepare a template containing the *cis-syn*-cyclobutane dimer of ^mCT. Through the use of single-hit and multiple-hit competition assays, the catalytic core of pol η was found to insert dGMP opposite the ^mC of the CPD with about a 120:1 selectivity relative to dAMP. No significant insertion of dTTP or dCMP was detected. The high fidelity of nonmutagenic insertion opposite the ^mC of the CPD provides strong support for the deamination–bypass mechanism for the origin of sunlight induced C → T mutations.

Sunlight is a major epidemiological risk factor for skin cancers. In basal cell and squamous cell carcinomas, the most common types of skin cancer, the p53 tumor suppressor gene exhibits a very high percentage of C→T transition mutations at dipyrimidine sites, including the tandem CC→TT mutation (1–5). Most C→T mutation hotspots occur at 5'-PyCG sites where the C is methylated at the 5 position (6–8). Previous studies of solar UV-induced mouse skin tumors indicate that a large percentage (30–50%) of these mutations are due to cyclobutane pyrimidine dimer (CPD¹) photoproducts that form abundantly in sunlight at these sites and are slowly repaired (9, 10). Furthermore, CPD formation in sunlight is enhanced 15-fold at 5'-PyCG sites in the p53 gene by the methylation of C (11). A comparison of sunlight-induced mutation spectra of the *cII* and *lacI* transgenes as well as the p53 gene in skin tumors indicates that 5-methylcytosine (^mC) is involved in 25–40% of all mutations in all three systems and that cyclobutane dipyrimidine dimers are responsible for a considerable fraction of these mutations (12). Whereas C and ^mC are very stable, C and ^mC in a CPD are unstable and can readily deaminate to U or T, respectively, in a matter of hours or days (13–16) (Figure 1). The facile deamination of C and ^mC in CPDs suggests that UV-induced C and ^mC to T mutations at dipyrimidine sites arise from the insertion of A opposite the U or T of a deaminated C or ^mC-containing CPD (the deamination–bypass mechanism). (17–19) (Figure 1).

In eukaryotic cells, the bypass of *cis-syn*-pyrimidine dimers (CPDs) involves polymerase η (20, 21), a member of the pol Y family of DNA damage bypass polymerases (22–25). Mutations in human pol η are responsible for the variant form of xeroderma pigmentosum (XP-V), a genetic disease that predisposes patients to an increased risk of skin cancer (26–28). Cells from XP-V individuals are deficient in UV-damaged DNA replication and are hypermutable to UV light, suggesting that pol η suppresses UV-induced mutations by synthesizing past cyclobutane dimers in an error free manner. Both yeast and human pol η efficiently bypass TT CPDs in a nonmutagenic manner by incorporating two As opposite the two Ts of the dimer (26, 29). Evidence for error-free bypass in vivo comes from mutagenesis studies with a plasmid bearing a site-specific TT CPD in yeast strains deleted for various polymerases (20). It is thought that yeast pol η also catalyzes the error-free bypass of C-containing CPDs because UV-induced C→T mutations in yeast occur primarily at the 3'-C of TC and CC sites, and the incidence of these mutations is about 5-fold higher in the Rad30 Δ yeast strain than in the wild type (30). The results in yeast are also consistent with an observation that a site-specific C-containing dimer was replicated with >95% accuracy in *E. coli* under SOS conditions (31) in which it is presumed that pol V, another member of the pol Y family, is involved. Although the selectivity of nucleotide insertion opposite the TT CPD by both yeast and human pol η (32–36) and by pol V (37) has been well characterized in vitro, determining the selectivity of nucleotide insertion opposite C-containing CPDs in vitro presents a significant challenge because of their instability and has not yet been reported.

Without knowing the precise nucleotide insertion specificity opposite a C or ^mC in a CPD, the possibility remains that the mispairing of C or ^mC with A also contributes to

[†] This work was supported by NIH Grant CA40463 (to J.S.T.).

* Corresponding author. Phone: (314) 935-6721. Fax: (314) 935-4481. E-mail: taylor@wustl.edu.

¹ Abbreviations: CPD, cyclobutane pyrimidine dimer; ESI, electrospray ionization; ^mC, 5-methylcytosine; MS/MS, tandem mass spectrometry; pol η , polymerase η .

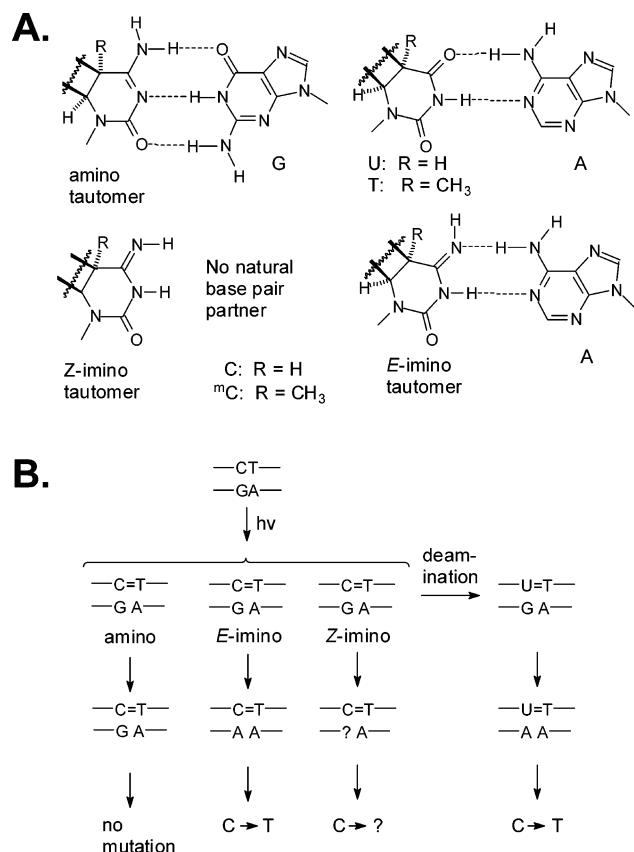


FIGURE 1: Mutagenic properties of C and ^mC in a *cis-syn* dimer and their deamination products, U and T, respectively. (A) The major tautomers of C and ^mC in a *cis-syn* dimer and their base pairing properties compared to their deamination products U and T. (B) Mutagenic consequences of the base pairing properties of the tautomers of C in a dimer and their deamination product, U. The same pertains to the tautomers of ^mC and their deamination product T.

UV-induced C and ^mC to T transitions. Such mispairing could explain the formation of C to T mutations observed at dipyrimidine sites in UV-irradiated DNA that are not given time to deaminate (38, 39). The mispairing of C in a dimer might occur at a greater frequency for a native C because saturation of the 5,6 double bond of C increases the fraction of imino tautomers, the *E*-isomer of which has the same base pairing properties as that of T (40) (Figure 1). Saturation of the 5,6 double bond of C results in a loss of aromatic resonance energy that would otherwise stabilize the amino tautomer of C and thus increases the fraction of the imino tautomer. Spectroscopic and *pK_a* measurements of 5,6-dihydrocytosine show that it predominantly adopts the amino tautomeric form in water but exists as a mixture of amino and imino tautomers in nonpolar solvents (40). Theoretical studies on *cis-syn*-pyrimidine dimers, however, predict that the imino tautomer of cytosine is more stable than the amino tautomer in the gas phase and that it is further stabilized in water (41). Both experimental and theoretical work suggest that some fraction of C in a dimer could adopt the *E*-imino tautomeric form and direct the insertion of A.

Herein we report the preparation and characterization of templates containing the *cis-syn*-cyclobutane dimer of ^mCT and the selectivity of dAMP and dGMP insertion opposite the ^mC in this dimer by the catalytic core of yeast pol eta. We found that dGMP is inserted with >99% selectivity

relative to dAMP. This observation suggests that most ^mC to T and possibly C to T mutations must arise from a deamination–bypass mechanism.

MATERIALS AND METHODS

Enzymes, Substrates, and Equipment. 5-Methyldeoxycytidine-containing template ODNs were prepared by automated DNA synthesis on an Expedite 8909 synthesis machine (PE Biosystems) with 5-methyldeoxycytidine-CE phosphoramidite from Glen Research and all other nucleoside phosphoramidites and CPG columns from PE Biosystems. Primer ODNs were prepared by Integrated DNA Technologies, Inc. and purified by 15% denaturing PAGE. Purification of the ^mCT-containing ODN was carried out on an Xterra MS C18 column (4.6 × 250 mm, 3.5 μm particle size and 300 Å pore size) from Waters, with a Beckman 126 solvent delivery module and a 168 detector HPLC system. T4 polynucleotide kinase was purchased from New England Biolabs, [γ -³²P] ATP from Amersham, and dNTPs from Invitrogen. All other standard reagents were from Sigma. Mass spectrometry was carried out on a Classic LCQ ion-trap mass spectrometer (Finnigan, San Jose, CA). The catalytic core of yeast pol η with a 6×His tag on its N-terminal was purified as previously described (42).

Preparation of a DNA Template Containing a *cis-syn*-^mC=T CPD. The 14-mer ODN d(GTA^mCTATGAGGTGC-3') was synthesized by standard automated solid-phase phosphoramidite synthesis and purified by reverse phase HPLC with 90 min 0–20% gradient of acetonitrile in 50 mM aqueous triethylammonium (pH 6.5). After lyophilization of the appropriate HPLC fractions, the ODN was resuspended in 300 μL of distilled water and placed into a 5 mm NMR tube, degassed with a stream of argon for 5 min. The tube was then strapped to the outside of a Pyrex immersion well reactor (Ace Glass) containing a Hanovia 450 W medium-pressure mercury vapor arc lamp and irradiated for 1.5 h at a distance of 2–3 cm while immersed in an ice bath. The reaction mixture was then immediately subjected to HPLC purification at room temperature with sequential 1 mL/min linear gradients of 0–10% (5 min), 10–15% (40 min), and 15–30% (10 min) acetonitrile in 100 mM aqueous triethylammonium acetate solution (pH 6.5). The collected fractions were immediately frozen on dry ice and then lyophilized to dryness and stored at –20 °C for further analysis. This procedure resulted in a sample of the ^mC=T 14-mer that was about 20% deaminated.

In a second procedure designed to reduce the deamination of the purified sample, 30 μg of DNA in 90 μL of 10 mM Tris (pH 8.8) was irradiated for 55 min on a piece of Saran wrap on a 302 nm transilluminator at 4 °C in a cold room. HPLC purification was carried out with 50 mM triethylamine-acetate at pH 8.0 in place of the pH 6.5 solution used before to yield about 1.9 μg of the *cis-syn* dimer eluting in 1 mL of about 10% acetonitrile. This sample was not lyophilized but was stored at –20 °C prior to use.

Preparation of a DNA Template Containing the *cis-syn* T=T Dimer. The pH of the ^mC=T 14-mer sample was adjusted to pH 7.0 by adding HCl and heated for 17 h at 57 °C to promote complete deamination.

DNA Photoproduct Identification and Characterization by Mass Spectrometry. The fractions corresponding to the major

photoproduct peaks from the HPLC purification of the ${}^m\text{C}=\text{T}$ 14-mer prepared by the first method were redissolved in distilled water and analyzed by an enzyme-coupled mass spectrometry assay (43, 44). In a typical assay, 1 μL of a 1 unit/ μL aqueous solution of nuclease P1 was added to a 30 μL aliquot of the ODN sample and incubated at room temperature for 3 min, then cooled on ice, and immediately analyzed by ESI coupled to MS/MS. MS/MS data were acquired on the selected $[\text{M} - \text{H}]$ ions. To select both the deaminated and undeaminated components for fragmentation, the mass width for precursor selection was set at 5–6 m/z units.

Deamination Rates by a Single-Hit Kinetic Assay. The ${}^m\text{C}=\text{T}$ 14-mer template (60 nM) prepared by the first method was adjusted to pH 8.2 with Tris base (10 mM) and incubated at 4, 23, 39, or 50 $^{\circ}\text{C}$. Aliquots (5 μL) were removed at various times and quickly frozen on dry ice before storing overnight at -70°C . All subsequent steps were performed in a cold room (4 $^{\circ}\text{C}$). To each of the 5 μL aliquots was added 5 μL of 20 nM 5'-[${}^{32}\text{P}$]-end-labeled primer, 20 mM Tris-HCl at pH 7.5, and 10 mM DTT and allowed to anneal for 10 min before the addition of polymerase η (300 nM). Each sample was incubated for an additional 7 min before initiating the single-hit synthesis by the addition 1:1 dATP–dGTP (200 μM each) containing 10 mM MgCl_2 , 10 mM Tris-HCl at pH 7.5, in 30 μL 10 mg/mL sonicated/denatured salmon sperm DNA as a polymerase trap. The synthesis reaction was quenched after 10 s by the addition of 80 μL of formamide containing 0.1% xylene cyanol, 0.2% SDS, 25 mM EDTA, and 1 μg of cold primer (stop mix). The samples were then heated at 100 $^{\circ}\text{C}$ for 10 min before loading on a 40 cm \times 0.4 mm 10% polyacrylamide gel containing 25 mM citrate at pH 3.5, which was the same as the reservoir buffer. The gel was polymerized by adding 400 μL of ferrous sulfate (250 mg/100 mL), 400 μL of 10% ascorbate, and 120 μL of 3% hydrogen peroxide. The gel was run at 2000 V until the xylene–cyanol dye marker reached 25 cm (about 3 h).

Analysis of the Deamination Rate Data. For the analysis of the single-hit competition assay, we assumed that at equal concentrations of dGTP and dATP only dGMP would be introduced in a significant amount opposite that of the ${}^m\text{C}=\text{T}$ CPD that was in the amino tautomeric form (F_E). Conversely, we assumed that dAMP would be inserted opposite the *E*-imino tautomeric form of the C and any T that results from the deamination of the C. We also assumed that the ${}^m\text{C}$ of the CPD would deaminate by a 1st order process, and that some fraction (F_T) of the original CPD would be present as the deaminated product at zero time. Thus, the fraction of dGMP inserted, $\text{G}/(\text{G} + \text{A})$, as a function of time can be expressed by $\ln[\text{G}/(\text{G} + \text{A})] = \ln[\text{F}_\text{E} \cdot (1 - \text{F}_\text{T})] - kt$. At zero time, $\ln[(\text{G}/\text{G} + \text{A})]_0$ is equal to the y intercept, from which the fraction of A inserted opposite ${}^m\text{C}=\text{T}$ is equal to $1 - [\text{G}/(\text{G} + \text{A})]_0 - \text{F}_\text{T}$.

Competitive Insertion Assays. These experiments were generally carried out as described above. For the single-hit synthesis, 5 nM primer/template, 5 mM DTT, 10 mM Tris-HCl at pH 7.5, and 500 nM pol η in 10 μL were preincubated for 7 min at 4 $^{\circ}\text{C}$ before adding 300 μg of sonicated and denatured salmon sperm DNA containing 10 mM MgCl_2 and the indicated concentration of nucleotide in 30 μL of 10 mM Tris-HCl at pH 7.5. After 10 s, the reactions were quenched

10mer	5'-GCACCTCATA-3'
10A	5'-GCACCTCATAA-3'
10G	5'-GCACCTCATAG-3'
14A	5'-GCACCTCATAATAC-3'
14G	5'-GCACCTCATAGTAC-3'
14 ${}^m\text{CT}$	3'-CGTGGAGTAT ${}^m\text{CATG}$ -5'
14 ${}^m\text{C}=\text{T}$	3'-CGTGGAGTAT ${}^m\text{CATG}$ -5'
14T=T	3'-CGTGGAGTAT=TATG-5'

FIGURE 2: Oligodeoxynucleotides used in this study.

with 80 μL of stop mix. For reactions under multiple-hit conditions, 5 nM primer/template, 500 μM each of dNTP, 10 mM MgCl_2 , 5 mM DTT, 10 mM Tris-HCl at pH 7.5, and 500 nM pol η were incubated at 4 $^{\circ}\text{C}$. At the specified time or times, a 10 μL aliquot was removed and added to a tube containing 300 μg of sonicated and denatured salmon sperm DNA before quenching the reaction with 80 μL of stop mix.

RESULTS

Design of the Dimer-Containing Templates. Because there are no DNA synthesis building blocks available for C-containing CPDs, the required substrate had to be prepared by the irradiation of an ODN followed by HPLC purification (31). Based on our experience, the ODN had to be about 15 nucleotides or less in length and contain a single dipyrimidine photoproduct site to enable the desired C-containing cis-syn CPD to be separated from the other dipyrimidine photoproducts and their deamination products by HPLC. Furthermore, the ODN had to be long enough to form a suitable template primer substrate for pol η . To minimize deamination during purification, we made use of the observation that C5 methylation reduces the rate of deamination of the C in dipyrimidine photoproducts (16, 45). Taking into account these criteria as well as the physical and enzymatic data we have accumulated on the thymine dimer embedded within the d(-GTATTATG-) sequence context, we prepared the CPD of the 14-mer sequence d(GTA ${}^m\text{CTATGAGGTGC}$) (Figure 2). This template is also long enough to be used with a 10-mer primer, which is sufficiently long for standing start kinetics assays (42). We also attempted to prepare the T= ${}^m\text{C}$ CPD of the same sequence but were unsuccessful at identifying and isolating the desired product.

Preparation and Characterization of cis-syn-5-Methylcytosine Cyclobutane Dimer-Containing 14-mers. In our first attempt, we irradiated the ${}^m\text{CT}$ 14-mer with medium-pressure mercury arc light in a Pyrex tube that was immersed in an ice–water bath to minimize the amount of deamination. The reaction mixture was then purified by reverse phase HPLC at room temperature (Figure 3A) and the various fractions cooled immediately on dry ice and then concentrated to dryness in vacuum in a centrifugal evaporator. The desired cis-syn dimer product was identified by mass spectral analysis after nuclease P1 digestion of the individual HPLC fractions. Nuclease P1 digests dipyrimidine photoproduct-containing ODNs to trinucleotides of the form pd(Py)[PyN], which can be assigned to a specific photoproduct on the basis of the characteristic fragment ions produced (43). The extent of deamination of the dimer could be estimated by the mass of the $[\text{M}-\text{Ade}-\text{H}]^-$ fragment ion of the trinucleotide digestion product, which increases by one, from 802 to 803, following deamination (Figure 3B).

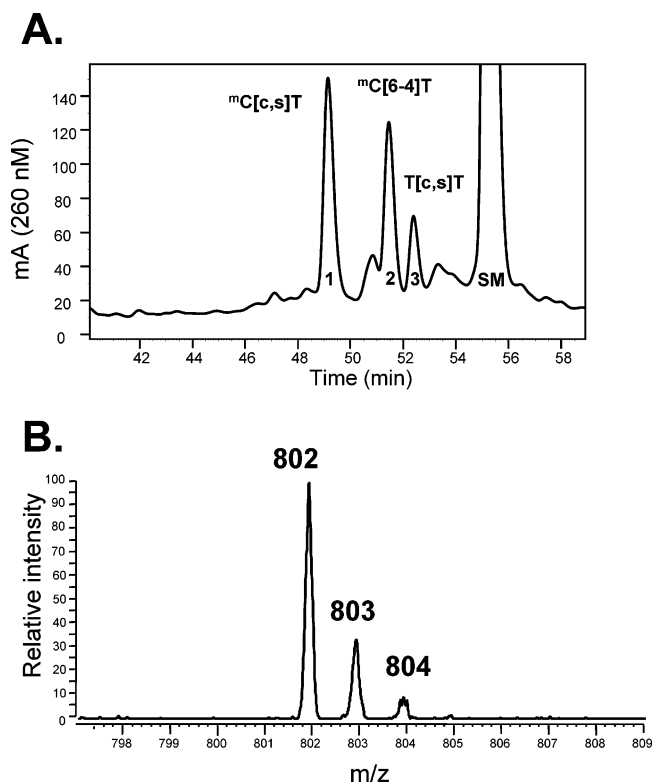


FIGURE 3: Analysis of the UV irradiation products of $14mCT$, $d(GTA^mCTATGAGGTGC)$. (A) HPLC analysis of the photoproduct mixture with a shallow gradient that allows the resolution of all of the major products. (B) Zoom scan analysis of the m/z 802–804 ion peaks in the nuclease P1-coupled MS/MS spectrum of the fraction corresponding to the *cis-syn* dimer of mCT with a mass window of 5 centered on the m/z 803 ion.

Three major products with retention times of 49, 51.5, and 52.5 min were detected by HPLC, all of which yielded trinucleotide products upon nuclease P1 digestion. The first product to elute was assigned to the *cis-syn*-cyclobutane dimer of mCT on the basis of the presence of a single major ion at m/z 802, which is characteristic of both the *cis-syn* and (6-4) products of mCT (Figure 4A), and the absence of a significant ion at m/z 825 ion, which is characteristic of the (6-4) product (43). The second peak was assigned to the (6-4) product of mCT on the basis of the presence of both of these ions (Figure 4C), whereas the third peak was assigned to the *cis-syn* dimer of TT on the basis of the presence of an m/z 803 ion and the absence of an m/z 825 ion.

As further confirmation of the assignments, the product assigned as the *cis-syn* dimer of mCT slowly converted to the product eluting at 21.7 min, which corresponds to the *cis-syn* dimer of TT , and gained one unit of mass (Figure 5). In contrast, the product assigned as the (6-4) product of mCT did not gain a unit of mass upon incubation under the same conditions (data not shown), which is consistent with the slow deamination rate of the (6-4) product of $d(mCpT)$ (45). The ODN containing the *cis-syn* dimer of mCT contained about $7 \pm 1\%$ of the deamination product on the basis of the ratio of the 802 and 803 peaks in four separate MS determinations with a mass window of 5 amu. This estimate, however, assumes that both the $mC=TA$ and $T=TA$ products have the same response factor and are produced with equal rates or in quantitative yield during the degradation of the ODN by nuclease P1, which may not be true.

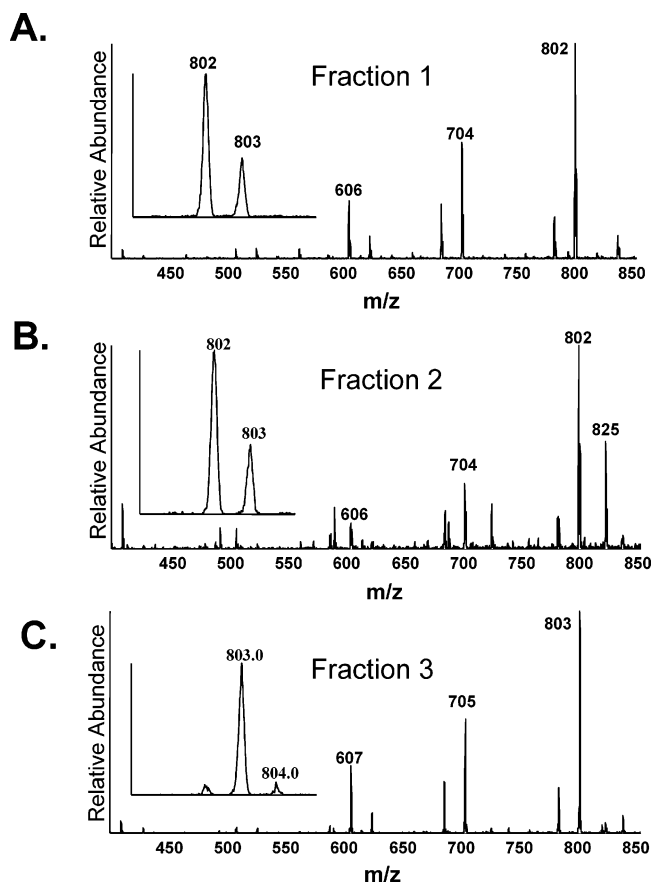


FIGURE 4: Nuclease P1-coupled ESI-MS/MS mass spectra of the three major irradiation products of $d(GTA^mCTATGAGGTGC)$. (A) The MS of HPLC peak one corresponding to the *cis-syn* dimer of mCT (A1: parent ion $m/z = 937$, full MS; A2: zoom scan at $m/z = 802$). (B) Spectra of HPLC peak two corresponding to the (6-4) product of mCT (A1: parent ion $m/z = 937$, full MS; A2: zoom scan at $m/z = 802$). (C) Spectra of HPLC peak three corresponding to the *cis-syn* dimer of TT (A1: parent ion $m/z = 937$, full MS; A2: zoom scan at $m/z = 802$). In the zoom scans, the m/z 804 was largely filtered out because of the use of too small a mass window and centering on the m/z 802 ion.

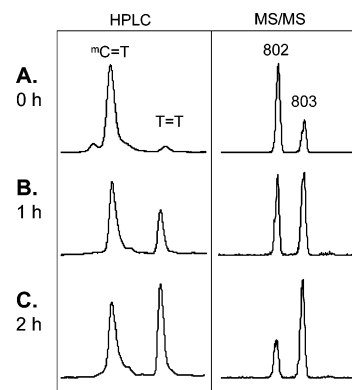


FIGURE 5: Deamination of the $mC=T$ CPD containing ODN. The ODN containing the *cis-syn* dimer of mCT prepared by the first method that eluted in peak one (Figure 3) was incubated at $37^\circ C$ for the times shown, frozen, and then thawed immediately before the HPLC and nuclease P1-coupled MS/MS assays; (A) 0 h of incubation, (B) 1 h of incubation, and (C) 2 h of incubation. The pH of the solution was not measured, but on the basis of the rate of deamination, the pH of the sample must have been below 7.

Single-Hit Competition Assay for dAMP and dGMP Insertion Opposite the $mC=T$ Dimer by pol η . We expected the amino tautomer of the mC in the $mC=T$ CPD to direct

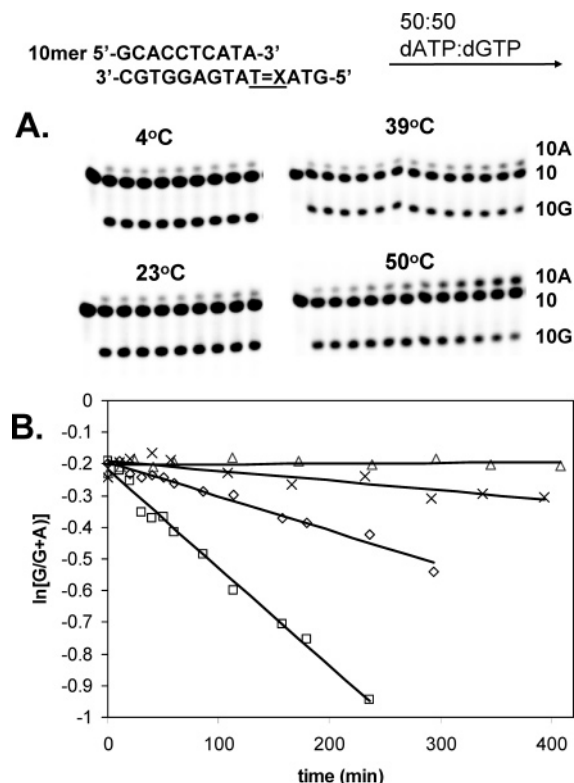


FIGURE 6: Temperature dependence of $mC=T$ CPD deamination at pH 8.2. (A) Single-hit nucleotide insertion competition assay carried out with a 1:1 mix of dGTP and dATP on the $mC=T$ CPD-containing 14-mer prepared by the first method as a function of time at the temperature shown. (B) Plot of $\ln[G/(G + A)]$ extension opposite the 5'-pyrimidine of the cis-syn dimer as a function of time for four different temperatures.

the insertion of dGMP and the *E*-imino tautomer and the T resulting from deamination to direct the insertion of dAMP. To determine the frequency of dAMP and dGMP insertion opposite the dimer site, we used a single-hit competition assay that we developed for this purpose. In this assay, the template primer is first incubated with a large excess of enzyme after which a 50:50 mixture of dATP and dGTP is added together with a large excess of sonicated calf thymus DNA to trap any free polymerase. Single-hit primer extension was performed at 4 °C to minimize deamination during the assay and to simplify gel analysis by limiting the number of nucleotides added to the primer. To resolve the products of dAMP and dGMP addition, we made use of polyacrylamide gel electrophoresis in the presence of 25 mM citrate at pH 3.5 (Figure 7A).

Temperature Dependence of $mC=T$ Dimer Deamination. When the single-hit competition reaction was carried out at 4 °C with the sample prepared by our first method, 20% of the insertion occurred with dAMP, which would be indicative of the presence of the *E*-imino tautomer and/or the deamination product. To confirm that no significant amount of deamination occurred during the assay, the primer template was incubated for various lengths of time at 4 °C at pH 8 prior to the addition of the polymerase (Figure 6). Under these conditions, we found the fraction of dAMP insertion remained constant with deamination time. We also carried out the incubation at higher temperatures to determine the effect of temperature on the deamination rate and to better estimate the amount of dAMP inserted at zero time by a linear fit to the equation $\ln[G/(G + A)] = \ln[G/G + A]_0 -$

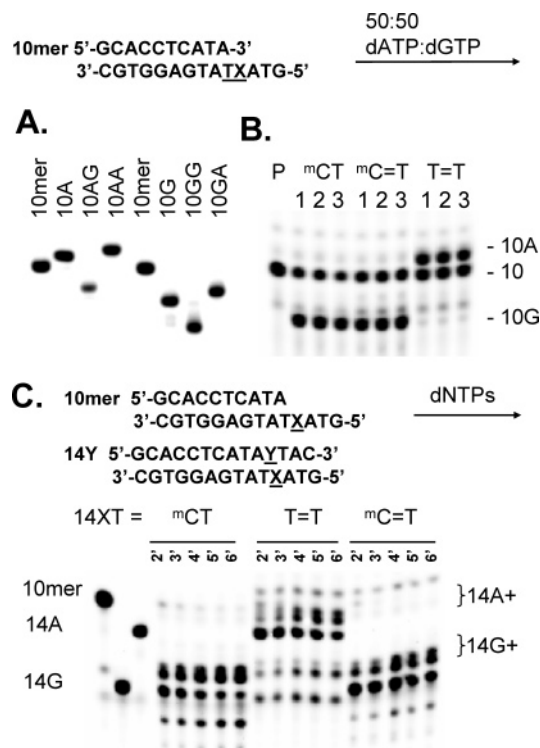


FIGURE 7: Comparison of nucleotide insertion selectivity opposite mCT , $mC=T$, and $T=T$. (A) Mobility of ODNs corresponding to the possible A and G extension products of the 10-mer primer opposite the dimer-containing 14-mer template ODN. (B) Single-hit nucleotide insertion competition assay carried out on the $mC=T$ CPD-containing ODN prepared by the second method, on its deamination product, the $T=T$ CPD, and on the undimerized mCT precursor. (C) Competition assay carried out under multiple-hit conditions with 500 μM of each dNTP on the $mC=T$ CPD-containing 14-mer prepared by the second method. C = primer alone, 1–7 = 20 s, 1, 2, 3, 5, and 10 min. The full-length products corresponding to A and G insertion opposite the mC of the dimer were identified by comparison to authentic synthetic ODNs (not shown).

k^*t (see Materials and Methods). From the intercepts of the line fits to this equation, the fraction of dGMP inserted at $t = 0$ at various temperatures was also found to be $80 \pm 1\%$. From the slope of the lines, the deamination rates were determined to be 0.00031, 0.0011, and 0.0031 min^{-1} at 23, 39, and 50 °C at pH 7.5, corresponding to deamination half-lives of 37, 10.5, and 3.7 h, respectively.

Frequency of dGMP and dAMP Insertion Opposite the mC of the $mC=T$ CPD. With the first sample of $mC=T$ dimer-containing DNA, we observed about 20% insertion of dAMP. To determine how much of the dAMP was being inserted opposite the $mC=T$ CPD, we needed to know how much $T=T$ CPD was present. Unfortunately, without a pure sample of $mC=T$, we could not calibrate analytical methods such as the nuclease P1-coupled MS assay. Rather than rely on an analytical method to determine the amount of $T=T$ dimer present, we decided to see if we could prepare a purer sample of the $mC=T$ CPD-containing ODN. A likely source of deamination may have been the triethylammonium buffer at pH 6.5 used in the HPLC purification step, which may have become even more acidic when it was evaporated. We therefore prepared a second sample in which the pH of the elution buffer was raised to 8.5, and the fraction containing the $mC=T$ CPD was immediately stored at -20 °C without evaporation. When these changes were made, $<1\%$ of dAMP

was observed to be inserted opposite the ^mC of the CPD in the single-hit competition experiment using equimolar dATP and dGTP (Figure 7B). The amount of dAMP inserted opposite the ^mC of the CPD was very similar to that inserted opposite the undimerized ^mC of ^mCT .

We also carried out the competition reaction under multiple hit conditions in the presence of all four dNTPs leading to complete extension to the end of the template. The products of complete extension could also be easily resolved on a 5% citrate PAGE gel allowing the quantification of the amount of dAMP and dGMP inserted opposite the dimer site (Figure 7C). At short reaction times, we primarily observed products corresponding to authentic 14-mers with either A or G inserted opposite the 5'-pyrimidine of the dimer. At longer reaction times, we observed slower migrating bands (14N+) that probably corresponded to products of blunt-end addition to the 14-mer, given that these bands appeared to increase at the expense of the 14-mer band. Assuming this to be the case, we found that <1% of the insertion opposite the 5'- ^mC of either the native or the dimerized ^mCT site occurred with dAMP in very good agreement with the single-hit competition results. Other products were also observed, which appeared to be in common between the ^mCT and $^m\text{C}=\text{T}$ substrates or between the T=T and $^m\text{C}=\text{T}$ substrates, which could have been the result of incomplete synthesis or misinsertion. Single-hit competition experiments (next section) suggest that these were not, however, due to the misinsertion of C or T opposite the ^mC of the dimer.

Selectivity of Nucleotide Insertion. To determine the selectivity of dGMP insertion opposite the ^mC of the CPD relative to dAMP, we varied the ratio of [dGTP] to [dATP] in a single-hit experiment (Figure 8A). When this experiment was carried out, the selectivity of dGMP insertion relative to dAMP insertion was calculated to be 120 ± 3 from the slope of a least-squares line fit to a plot of 10A/10G vs [dATP]/[dGTP] (Figure 8B) (46). We also carried out single-hit competition experiments between dGTP and dATP, and dTTP and dCTP under a single biased nucleotide ratio of 100:1 competitor–dGTP (Figure 8C). To assign the product bands, we carried out the primer extension of the product that would result from the insertion of the competitor or dGMP (10N or 10G) in the presence of both competing nucleotides. Whereas we could readily identify the product resulting from the insertion of dAMP in competition with dGMP, no products over the background could be detected resulting from the insertion of either dTMP or dCMP in competition with dGMP, indicating that they are much less efficiently inserted.

Single Nucleotide Insertion Experiments. We also examined the efficiency of dAMP and dGMP insertion under single nucleotide insertion conditions, in which a nucleotide does not have to compete with another nucleotide for insertion (Figure 9A). Surprisingly, the insertion of dAMP under single-hit conditions occurs more efficiently opposite ^mC in the CPD than opposite undamaged ^mC , and dGMP is inserted opposite the 5'-T of the T=T CPD. Likewise, under multiple-hit conditions, the insertion of dAMP opposite ^mC in the $^m\text{C}=\text{T}$ dimer reached 80% in 20 s, whereas it only reached 38% opposite undamaged ^mC . The insertion of dAMP opposite ^mC in the $^m\text{C}=\text{T}$ CPD appeared to be equal

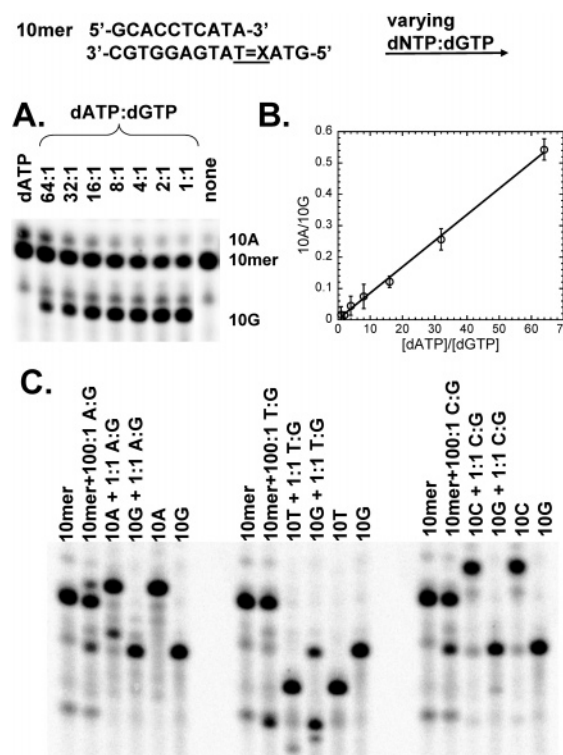


FIGURE 8: Selectivity of dGMP insertion opposite ^mC of $^m\text{C}=\text{T}$ relative to other nucleotides. (A) Results of single-hit nucleotide insertion with varying ratios of dATP/dGTP at a fixed dATP concentration of 100 μM . (B) Linear regression analysis of the ratio of products formed vs the dATP/dGTP ratio. (C) Results of single-hit nucleotide insertion with 100 μM dNTP (N = A, T, or C) and 1 μM dGTP along with authentic products resulting from the insertion N or G opposite the 5'- ^mC and their extension with 200 μM dNTP and 200 μM dGTP.

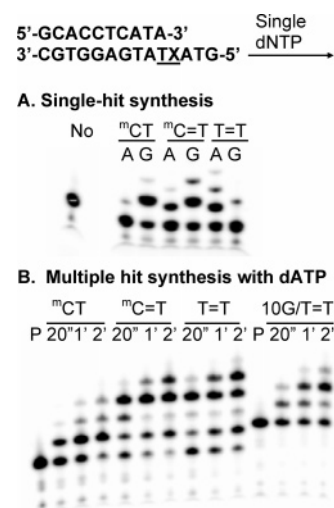


FIGURE 9: Single nucleotide insertion assays opposite ^mCT , $^m\text{C}=\text{T}$, and T=T. (A) Single-hit insertion assay carried out with either 500 μM dGTP or dATP. (B) Single nucleotide insertion assay carried out with 500 μM dATP under multiple-hit conditions.

to or even slightly more efficient than the insertion of dAMP opposite the 5'-T of the T=T dimer.

DISCUSSION

In human skin cancers, more than 30% of all mutations are C to T or CC to TT transitions at 5'-PyCG sites, and the origin of these transitions has been the subject of intense

speculation and investigation. The deamination–bypass mechanism (17, 18) is generally accepted as the origin of UV-induced mutations for which there is much evidence in both prokaryotes (38, 47–54) and eukaryotes (15, 39, 55). The most important lines of evidence are that (1) the C in a site-specific cis-syn T=C CPD codes primarily (>95%) as C in *E. coli* (31), (2) the level of UV-induced C to T mutations increases when irradiated DNA is allowed to stand prior to transfection into *E. coli* (52, 53) and human cells (39), (3) C- and ¹⁴C-containing CPDs deaminate within hours (13–16), and (4) T and U- and T-containing dimers direct the insertion of A by the CPD bypass polymerase pol V of *E. coli* (37) and pol η of yeast (29) and humans (56, 57).

Even at zero incubation time, however, C to T mutations are observed, which might arise from deamination of the dimers within the cell prior to trans-lesion synthesis. It is also possible that some C to T mutations arise from the insertion of A opposite the C in a dimer by a nontemplated transient abasic site-like mechanism as found for T7 polymerase (46, 58, 59) or by a tautomer-bypass mechanism (60, 61), or simply by a low fidelity mechanism.

In this study, we determined the extent to which dAMP is inserted opposite 5-methylcytosine in a cis-syn dimer by the catalytic core of yeast DNA polymerase pol η . Pol η has been proposed to suppress UV mutagenesis, by synthesizing past cis-syn-cyclobutane pyrimidine dimers in a nonmutagenic manner. In vitro studies have shown that yeast pol η inserts dAMP opposite the 5'-T of a cis-syn-thymine dimer in a highly nonmutagenic manner, making a transition or transversion error with a frequency of less than 0.5% (62). This agrees with our single-hit competition assay, which detected the insertion of <1% dGMP opposite the 5'-T of the dimer in the presence of equimolar dGTP and dATP (Figure 7B). Because the nucleotide insertion efficiency of pol η depends on H bonding in a Watson–Crick geometry (63, 64), we expected dGMP to be inserted opposite ¹⁴C of the cis-syn dimer in its amino tautomeric form and dATP opposite its E-imino tautomeric form with selectivity similar to that observed for dATP opposite the T in a TT dimer. In this study, we observed <1% insertion of dAMP opposite a highly pure sample of the ¹⁴C=T dimer in both single-hit and multiple-hit competition experiments (Figure 7B and C), consistent with the 0.5% expected if the ¹⁴C were exclusively in its amino tautomeric state. We also found that the selectivity of insertion corresponding to $(k_{\text{cat}}/K_M)_{\text{dGTP}}/(k_{\text{cat}}/K_M)_{\text{dATP}}$ was 120:1 for dGMP insertion relative to dAMP opposite ¹⁴C of the ¹⁴C=T CPD (Figure 8B). This selectivity is very similar to that of 217:1 for the insertion of dAMP relative to dGMP opposite a T=T CPD (62). No evidence was found for the competitive insertion of dTMP or dCMP (Figure 8C).

Interestingly, with single nucleotides under single-hit conditions, the insertion of dAMP opposite ¹⁴C of the ¹⁴C=T CPD occurred at a reproducibly higher frequency than opposite undimerized ¹⁴C or for the insertion of dGMP opposite the 5'-T of the T=T CPD (Figure 9A). The increased efficiency might be explained by the facile equilibration of the amino tautomer with a small amount of the E-imino tautomer, which could base pair with dATP in a Watson Crick geometry (Figure 1). The possible existence of the E-imino tautomer of ¹⁴C is consistent with the results of spectroscopic studies on dihydrocytosine (40), which like

the cis-syn dimer, no longer possesses a 5,6 double bond, and hence lacks aromaticity to stabilize the amino tautomer. The spectroscopic studies found that 4% of dihydrocytosine was present as the imino tautomer in water, whereas it was the exclusive tautomer in chloroform. It has also been found that 5,6-dihydrocytidine triphosphate can substitute for either CTP or UTP by RNA polymerases (65), and A is incorporated exclusively opposite a C6 methoxylamine adduct of C, which also contains a saturated 5,6 double bond (66).

Whereas the enhanced insertion of dAMP opposite mC in the CPD relative to undimerized mC under single nucleotide conditions suggests that the E-imino tautomer is able to equilibrate with the amino tautomer, the competition experiments suggest that the fraction of E-imino tautomer is very low. Although the active site of pol η appears to be hydrophobic, as judged by its preference to insert the hydrophobic pyrene nucleotide relative to A opposite a normal template T (67, 68), and should favor the imino tautomer, the amino group of the ¹⁴C in the dimer, which lies in the major groove, may be largely exposed to water which would favor the amino form. It is also possible that the 5-methyl group on C disfavors the E-imino tautomer more than the amino tautomer because of steric interactions.

CONCLUSIONS

We have shown within limits of detection that ¹⁴C located in the 5'-position of a cis-syn dipyrimidine dimer codes as C. These data lend further support to a deamination–bypass mechanism for UV-induced C→T mutations in which nucleotide insertion opposite the C in a dimer is largely nonmutagenic and requires deamination to significantly increase the insertion frequency of dAMP. It remains to be determined, however, the extent to which the coding properties of C in a dimer are modulated by the specific polymerase involved, the position of the C within the dimer and its methylation state, and the flanking sequence.

REFERENCES

1. Brash, D. E., Rudolph, J. A., Simon, J. A., Lin, A., McKenna, G. J., Baden, H. P., Halperin, A. J., and Ponten, J. (1991) A role for sunlight in skin cancer: UV-induced p53 mutations in squamous cell carcinoma, *Proc. Natl. Acad. Sci. U.S.A.* 88, 10124–10128.
2. Ziegler, A., Leffell, D. J., Kunala, S., Sharma, H. W., Gailani, M., Simon, J. A., Halperin, A. J., Baden, H. P., Shapiro, P. E., Bale, A. E., and Brash, D. E. (1993) Mutation hotspots due to sunlight in the p53 gene on nonmelanoma skin cancers, *Proc. Natl. Acad. Sci. U.S.A.* 90, 4216–4220.
3. Dumaz, N., van Kranen, H. J., de Vries, A., Berg, R. J., Wester, P. W., van Kreijl, C. F., Sarasin, A., Daya-Grosjean, L., and de Gruijl, F. R. (1997) The role of UV-B light in skin carcinogenesis through the analysis of p53 mutations in squamous cell carcinomas of hairless mice, *Carcinogenesis* 18, 897–904.
4. Ananthaswamy, H. N., Fourtanier, A., Evans, R. L., Tison, S., Medaisko, C., Ullrich, S. E., and Kripke, M. L. (1998) p53 Mutations in hairless SKH-hr1 mouse skin tumors induced by a solar simulator, *Photochem. Photobiol.* 67, 227–232.
5. Queille, S., Seite, S., Tison, S., Medaisko, C., Drougard, C., Fourtanier, A., Sarasin, A., and Daya-Grosjean, L. (1998) p53 Mutations in cutaneous lesions induced in the hairless mouse by a solar ultraviolet light simulator, *Mol. Carcinog.* 22, 167–174.
6. Denissenko, M. F., Chen, J. X., Tang, M. S., and Pfeifer, G. P. (1997) Cytosine methylation determines hot spots of DNA damage in the human P53 gene, *Proc. Natl. Acad. Sci. U.S.A.* 94, 3893–3898.
7. Pfeifer, G. P., Tang, M., and Denissenko, M. F. (2000) Mutation hotspots and DNA methylation, *Curr. Top. Microbiol. Immunol.* 249, 1–19.

8. You, Y. H., Li, C., and Pfeifer, G. P. (1999) Involvement of 5-methylcytosine in sunlight-induced mutagenesis, *J. Mol. Biol.* 293, 493–503.
9. Drouin, R., and Therrien, J. P. (1997) UVB-induced cyclobutane pyrimidine dimer frequency correlates with skin cancer mutational hotspots in p53, *Photochem. Photobiol.* 66, 719–26.
10. You, Y. H., Szabo, P. E., and Pfeifer, G. P. (2000) Cyclobutane pyrimidine dimers form preferentially at the major p53 mutational hotspot in UVB-induced mouse skin tumors, *Carcinogenesis* 21, 2113–2117.
11. Tommasi, S., Denissenko, M. F., and Pfeifer, G. P. (1997) Sunlight induces pyrimidine dimers preferentially at 5-methylcytosine bases, *Cancer Res.* 57, 4727–4730.
12. You, Y. H., and Pfeifer, G. P. (2001) Similarities in sunlight-induced mutational spectra of CpG-methylated transgenes and the p53 gene in skin cancer point to an important role of 5-methylcytosine residues in solar UV mutagenesis, *J. Mol. Biol.* 305, 389–399.
13. Setlow, R. B. (1966) Cyclobutane-type pyrimidine dimers in polynucleotides, *Science* 153, 379–386.
14. Lemaire, D. G. E., and Ruzsicska, B. P. (1993) Kinetic analysis of the deamination reactions of cyclobutane dimers of dTpdC and dCpdT, *Biochemistry* 32, 2525–2533.
15. Tu, Y., Dammann, R., and Pfeifer, G. P. (1998) Sequence and time-dependent deamination of cytosine bases in UVB-induced cyclobutane pyrimidine dimers in vivo, *J. Mol. Biol.* 284, 297–311.
16. Celewicz, L., Mayer, M., and Shetlar, M. D. (2005) The photochemistry of thymidyl(3′-5′)-5-methyl-2′-deoxycytidine in aqueous solution, *Photochem. Photobiol.* 81, 404–418.
17. Taylor, J.-S., and O’Day, C. L. (1990) Cis-syn thymine dimers are not absolute blocks to replication by DNA polymerase I of *Escherichia coli* in vitro, *Biochemistry* 29, 1624–1632.
18. Jiang, N., and Taylor, J.-S. (1993) In vivo evidence that UV-induced C[to]T mutations at dipyrimidine sites could result from the replicative bypass of cis-syn cyclobutane dimers or their deamination products, *Biochemistry* 32, 472–481.
19. Pfeifer, G. P., Tang, M. S., and Denissenko, M. F. (2000) Mutation hotspots and DNA methylation, *Curr. Top. Microbiol. Immunol.* 249, 1–19.
20. Gibbs, P. E., McDonald, J., Woodgate, R., and Lawrence, C. W. (2005) The relative roles in vivo of *Saccharomyces cerevisiae* Pol eta, Pol zeta, Rev1 protein and Pol32 in the bypass and mutation induction of an abasic site, T-T (6-4) photoadduct and T-T cis-syn cyclobutane dimer, *Genetics* 169, 575–582.
21. Lehmann, A. R. (2005) Replication of damaged DNA by translesion synthesis in human cells, *FEBS Lett.* 579, 873–876.
22. Burgers, P. M., Koonin, E. V., Bruford, E., Blanco, L., Burtis, K. C., Christman, M. F., Copeland, W. C., Friedberg, E. C., Hanaoka, F., Hinkle, D. C., Lawrence, C. W., Nakanishi, M., Ohmori, H., Prakash, L., Prakash, S., Reynaud, C. A., Sugino, A., Todo, T., Wang, Z., Weill, J. C., and Woodgate, R. (2001) Eukaryotic DNA polymerases: proposal for a revised nomenclature, *J. Biol. Chem.* 276, 43487–43490.
23. Ohmori, H., Friedberg, E. C., Fuchs, R. P., Goodman, M. F., Hanaoka, F., Hinkle, D., Kunkel, T. A., Lawrence, C. W., Livneh, Z., Nohmi, T., Prakash, L., Prakash, S., Todo, T., Walker, G. C., Wang, Z., and Woodgate, R. (2001) The Y-family of DNA polymerases, *Mol. Cell* 8, 7–8.
24. Yang, W. (2003) Damage repair DNA polymerases Y, *Curr. Opin. Struct. Biol.* 13, 23–30.
25. Yang, W. (2005) Portraits of a Y-family DNA polymerase, *FEBS Lett.* 579, 868–872.
26. Masutani, C., Kusumoto, R., and Hanaoka, F. (1999) The XPV (xeroderma pigmentosum variant) gene encodes human DNA Polymerase eta, *Nature* 399, 700.
27. Stary, A., Kannouche, P., Lehmann, A. R., and Sarasin, A. (2003) Role of DNA Polymerase η in the UV Mutation Spectrum in Human Cells, *J. Biol. Chem.* 278, 18767–18775.
28. Kannouche, P., and Stary, A. (2003) Xeroderma pigmentosum variant and error-prone DNA polymerases, *Biochimie* 85, 1123–1132.
29. Johnson, R. E., Prakash, S., and Prakash, L. (1999) Efficient bypass of a thymine-thymine dimer by yeast DNA polymerase, pol eta, *Science* 283, 1001–1004.
30. Yu, S. L., Johnson, R. E., Prakash, S., and Prakash, L. (2001) Requirement of DNA polymerase eta for error-free bypass of UV-induced CC and TC photoproducts, *Mol. Cell Biol.* 21, 185–188.
31. Horsfall, M. J., Borden, A., and Lawrence, C. W. (1997) Mutagenic properties of the T-C cyclobutane dimer, *J. Bacteriol.* 179, 2835–2839.
32. Masutani, C., Kusumoto, R., Iwai, S., and Hanaoka, F. (2000) Mechanisms of accurate translesion synthesis by human DNA polymerase eta, *EMBO J.* 19, 3100–3109.
33. Washington, M. T., Johnson, R. E., Prakash, L., and Prakash, S. (2001) Accuracy of lesion bypass by yeast and human DNA polymerase eta, *Proc. Natl. Acad. Sci. U.S.A.* 98, 8355–8360.
34. Washington, M. T., Prakash, L., and Prakash, S. (2001) Yeast DNA polymerase eta utilizes an induced-fit mechanism of nucleotide incorporation, *Cell* 107, 917–927.
35. Washington, M. T., Johnson, R. E., Prakash, S., and Prakash, L. (2001) Mismatch extension ability of yeast and human DNA polymerase eta, *J. Biol. Chem.* 276, 2263–2266.
36. McCulloch, S. D., Kokoska, R. J., Masutani, C., Iwai, S., Hanaoka, F., and Kunkel, T. A. (2004) Preferential cis-syn thymine dimer bypass by DNA polymerase eta occurs with biased fidelity, *Nature* 428, 97–100.
37. Tang, M., Pham, P., Shen, X., Taylor, J.-S., O’Donnell, M., Woodgate, R., and Goodman, M. F. (2000) Roles of *E. coli* DNA polymerases IV and V in lesion-targeted and untargeted SOS mutagenesis, *Nature* 404, 1014–1018.
38. Fix, D. (1986) Thermal resistance of UV-mutagenesis to photo-reactivation in *E. coli* B/r uvrA ung: estimate of activation energy and further analysis, *Mol. Gen. Genet.* 204, 452–456.
39. Lee, D.-H., and Pfeifer, G. P. (2003) Deamination of 5-methylcytosines within cyclobutane pyrimidine dimers is an important component of UVB mutagenesis, *J. Biol. Chem.* 278, 10314–10321.
40. Brown, D. M., and Hewlins, M. J. E. (1968) Dihydrocytosine and related compounds, *J. Chem. Soc. C* 2050–2055.
41. Danilov, V. I., Les, A., and Alderfer, J. L. (2001) A theoretical study of the cis-syn pyrimidine dimers in the gas phase and water cluster and a tautomer-bypass mechanism for the origin of UV-induced mutations, *J. Biomol. Struct. Dyn.* 19, 179–91.
42. Cannistraro, V. J., and Taylor, J. S. (2004) DNA-thumb interactions and processivity of T7 DNA polymerase in comparison to yeast polymerase eta, *J. Biol. Chem.* 279, 18288–18295.
43. Wang, Y., Taylor, J. S., and Gross, M. L. (1999) Nuclease P1 digestion combined with tandem mass spectrometry for the structure determination of DNA photoproducts, *Chem. Res. Toxicol.* 12, 1077–1082.
44. Wang, Y., Gross, M. L., and Taylor, J. S. (2001) Use of a combined enzymatic digestion/ESI mass spectrometry assay to study the effect of TATA-binding protein on photoproduct formation in a TATA box, *Biochemistry* 40, 11785–11793.
45. Douki, T., and Cadet, J. (1994) Formation of cyclobutane dimers and (6-4) photoproducts upon far-UV photolysis of 5-methylcytosine-containing dinucleoside monophosphates, *Biochemistry* 33, 11942–11950.
46. Sun, L., Wang, M., Kool, E. T., and Taylor, J. S. (2000) Pyrene nucleotide as a mechanistic probe: Evidence for a transient abasic site-like intermediate in the bypass of dipyrimidine photoproducts by T7 DNA polymerase, *Biochemistry* 39, 14603–14610.
47. Fix, D., and Bockrath, R. (1981) Thermal resistance to photoreactivation of specific mutations potentiated in *E. coli* B/r ung by ultraviolet light, *Mol. Gen. Genet.* 182, 7–11.
48. Fix, D., and Bockrath, R. (1983) Targeted mutation at cytosine-containing pyrimidine dimers: Studies of *Escherichia coli* B/r with acetophenone and 313-nm light, *Proc. Natl. Acad. Sci. U.S.A.* 80, 4446–4449.
49. Bockrath, R., Ruiz-Rubio, M., and Bridges, B. A. (1987) Specificity of mutation by UV light and delayed photoreversal in umuC-defective *Escherichia coli* K-12: A targeting intermediate at pyrimidine dimers, *J. Bacteriol.* 169, 1410–1416.
50. Ruiz-Rubio, M., and Bockrath, R. (1989) On the possible role of cytosine deamination in delayed photoreversal mutagenesis targeted at thymine-cytosine dimers in *E. coli*, *Mutat. Res.* 210, 93–102.
51. Tessman, I., Liu, S.-K., and Kennedy, M. A. (1992) Mechanism of SOS mutagenesis of UV-irradiated DNA: Mostly error-free processing of deaminated cytosine, *Proc. Natl. Acad. Sci. U.S.A.* 89, 1159–1163.
52. Barak, Y., Cohen-Fix, O., and Livneh, Z. (1995) Deamination of cytosine-containing pyrimidine photodimers in UV-irradiated DNA, *J. Biol. Chem.* 270, 24174–24179.

53. Peng, W., and Shaw, B. R. (1996) Accelerated deamination of cytosine residues in UV-induced cyclobutane pyrimidine dimers leads to CC→TT transitions, *Biochemistry* 35, 10172–10181.
54. Burger, A., Fix, D., Liu, H., Hays, J., and Bockrath, R. (2003) In vivo deamination of cytosine-containing cyclobutane pyrimidine dimers in *E. coli*: A feasible part of UV-mutagenesis, *Mutat. Res.* 522, 145–156.
55. Pfeifer, G. P., You, Y.-H., and Besaratinia, A. (2005) Mutations induced by ultraviolet light, *Mutat. Res.* 571, 19–31.
56. Masutani, C., Araki, M., Yamada, A., Kusumoto, R., Nogimori, T., Maekawa, T., Iwai, S., and Hanaoka, F. (1999) Xeroderma pigmentosum variant (XP-V) correcting protein from HeLa cells has a thymine dimer bypass DNA polymerase activity, *EMBO J.* 18, 3491–3501.
57. Takasawa, K., Masutani, C., Hanaoka, F., and Iwai, S. (2004) Chemical synthesis and translesion replication of a cis-syn cyclobutane thymine-uracil dimer, *Nucleic Acids Res.* 32, 1738–1745.
58. Smith, C. A., Baeten, J., and Taylor, J. S. (1998) The ability of a variety of polymerases to synthesize past site-specific cis-syn, trans-syn-II, (6-4), and dewar photoproducts of thymidyl- (3'→5')-thymidine, *J. Biol. Chem.* 273, 21933–21940.
59. Taylor, J. S. (2002) New structural and mechanistic insight into the A-rule and the instructional and noninstructional behavior of DNA photoproducts and other lesions, *Mutat. Res.* 510, 55–70.
60. Bockrath, R., and Cheung, M. K. (1973) The role of nutrient broth supplementation in UV mutagenesis of *E. coli*, *Mutat. Res.* 19, 23–32.
61. Person, S., McCloskey, J. A., Snipes, W., and Bockrath, R. C. (1974) Ultraviolet mutagenesis and its repair in an *Escherichia coli* strain containing a nonsense codon, *Genetics* 78, 1035–1049.
62. Washington, M. T., Johnson, R. E., Prakash, S., and Prakash, L. (2000) Accuracy of thymine-thymine dimer bypass by *Saccharomyces cerevisiae* DNA polymerase η , *Proc. Natl. Acad. Sci. U.S.A.* 97, 3094–3099.
63. Washington, M. T., Helquist, S. A., Kool, E. T., Prakash, L., and Prakash, S. (2003) Requirement of Watson–Crick hydrogen bonding for DNA synthesis by yeast DNA polymerase η , *Mol. Cell. Biol.* 23, 5107–5112.
64. Hwang, H., and Taylor, J. S. (2005) Evidence for Watson–Crick and not Hoogsteen or Wobble base pairing in the selection of nucleotides for insertion opposite pyrimidines and a thymine dimer by yeast DNA pol η , *Biochemistry* 44, 4850–4860.
65. Grossman, L., Kato, K., and Orce, L. (1966) Error induction in the RNA polymerase system of *M. lysodeikticus* by reduced pyrimidine nucleoside triphosphates, *Fed. Proc.* 25, 276.
66. Phillips, J. H., and Brown, D. M. (1966) The efficiency of induction of mutations by hydroxylamine, *J. Mol. Biol.* 21, 405–419.
67. Sun, L., Zhang, K., Zhou, L., Hohler, P., Kool, E. T., Yuan, F., Wang, Z., and Taylor, J. S. (2003) Yeast Pol η holds a cis-syn thymine dimer loosely in the active site during elongation opposite the 3'-T of the dimer, but tightly opposite the 5'-T, *Biochemistry* 42, 9431–9437.
68. Hwang, H., and Taylor, J. S. (2004) Role of base stacking and sequence context in the inhibition of yeast DNA polymerase η by pyrene nucleotide, *Biochemistry* 43, 14612–23.

BI0602009